



Influence of Radiation on the Squeezed flow of Copper-Water Nanofluid between Parallel Plates in Presence of Porous Medium and Magnetic Field

T.Chandrapushpam¹, K. Janagi², S. Ruth Kethsial³

^{1,3}Nehru Arts and Science College, Coimbatore, Tamilnadu, India.

²Department of Mathematics, KPR Institute of Engineering and Technology, Arasur, Tamilnadu, India.

Email ID: temathimalar@gmail.com¹, k.janagi@kpriet.ac.in², nascruthkethsial@nehrucolleges.com³

Abstract

This article highlights the outcome of the investigation on the squeezed flow of copper-water nanofluid between two moving parallel plates filled with a porous medium in presence of a magnetic field using a semi analytical method called Differential Transform Method (DTM). In this study, the influence of radiation parameter and the use of porous medium are considered along with other usual parameters. Impact of physical parameters like squeezing number, Hartmann number, Darcy number, and Biot number on velocity and energy distributions are presented and examined with the help of graphs and tables. From this study it is apparent that by increasing Biot number, radiation number, and Darcy number, the energy distribution attains a greater level.

Keywords: Squeezing flow; Radiation, Darcy number, Differential Transform Method, Biot number

1. Introduction

Flow of fluid between two parallel objects approaching each other- commonly referred to as squeezing flow-deserves more detailed research. In many of the engineering models, existence of squeezing flow is an undeniable fact in both non-Newtonian and Newtonian fluids and these applications are apparent in food processing, chocolate fillers, hydraulic lifts, polymers processing, moving pistons, electric motors, compression, power transmission squeezed film, etc. In 1874, Stefan initiated the pioneering work on squeeze flow and this was followed by Reynolds in 1886. After their work, many researchers have taken considerable and consistent efforts in modeling squeezing flow. Owing to its extensive industrial applications, in the past two decades logical and systematic investigations have been steadily increasing on squeeze flow. Engmann et al. [1] established that squeeze flow is an adaptable and consistent process of rheological description. Considerable insights in fluid flow behavior under different conditions in the field of MHD were provided through many researches [2-8]. Siddiqui et al. [9] evaluated the flow of viscous MHD fluid squeezed between two parallel infinite plates in existence of a magnetic field via homotopy perturbation method. Saadatmandi et al. [10] and

Ran et al. [11] explored the flow of a Newtonian incompressible fluid which is axisymmetric and squeezed between parallel plates. Rashidi et al. [12] solved the problem for circular plates. Researches on heat transfer during squeezing flow have been improving rapidly owing to its wide importance in many fields like science and industrial engineering. Heat transmission happens in various systems viz. electronic devices, heat exchange machines, automobiles, refrigerators, and so on. Size reduction in heat exchangers helps to increase the heat conductive property and hence miniaturization techniques of recent days are very much constructive. Technology provided us newer materials with more advantageous properties. One of the newer materials with desirable features along with high heat conductivity property is nanofluid and this helps in improving the design of heat exchangers. Heat transfer and thermal radiation play a major character in illustrating engineering design and development and therefore researches on finding the influences of thermal radiation in fluid flow are increasing constantly. A significant number of researchers investigated the flow behavior of nanofluids in different fields under different conditions which offer a significant insight as in [13-15]. Many authors discussed the flow behavior of

fluids along with convective boundary layer conditions. Considering these boundary conditions, Noghrehabadi et al. [16,17] explored the consequence of the slip boundary layer condition on the heat transmit features of stretching surface, and the influence of heat absorption/generation over the stretching plane. Hayat et al. [18] analyzed the flow of nanofluids over a stretching sheet through a porous medium. The nanofluid flow on the boundary layer over a stretching surface was studied by Makinde and Aziz [19]. Khan and Gorla [20] studied the performance of power-law nanofluids over a stretching surface in a nanofluid with existing invariable nanoparticle concentration of the surface. Aziz and Khan [21] applied a combined numerical and similarity approach to analyze the natural convective boundary layer flow of a nanofluid over a vertical plate. Mkwizu and Makinde [22] presented the joint influences of Brownian motion, thermophoresis, and variable viscosity on entropy generation in a water-based nanofluid flow between two parallel plates. Fluid flows through porous media take a significant role in many fields of mechanical applications, earth and environmental sciences. Various impacts of chemical reaction and other fluid flow parameters on MHD joint convection stagnation-point stream through a porous medium were discussed by many authors [23, 24, 25] using analytical and numerical methods. The solution for vertical plate embedded in a highly porous medium with effect of heat and mass transfer was evaluated by Karthikeyan et al. [26]. Various studies were carried out on squeeze flow of fluid between parallel objects filled with porous medium under different conditions [27-32]. The foremost intend of the current study is to explore the influence of radiative heat transfer in the flow behavior of a copper-water nanofluid squeezed between two parallel plates filled with porous medium along with externally applied magnetic field. To predict the flow behavior in converting the primary equations – Partial Differential Equations (PDE) to Ordinary Differential Equations (ODE), similarity transformation is applied. In recent studies various analytical and numerical methods have been adopted by researchers in analyzing the flow processes which

is a nonlinear problem. In the course of current study, an analytical method called Differential Transformation Method (DTM) which enables the convergent solution while resolving the resultant ODEs. Impacts of physical parameters are demonstrated and the outcomes are analyzed with the results of earlier investigators [15].

1.1. Formulation of the Problem

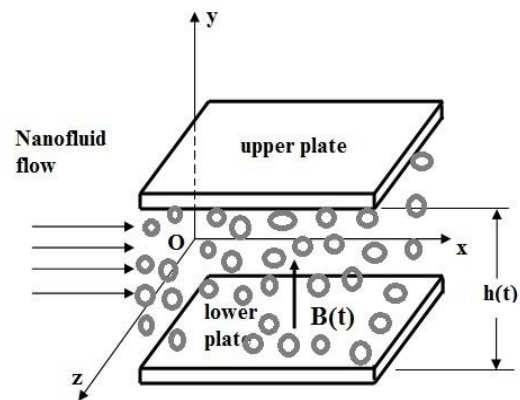


Figure 1 Fluid Flow System- Model

The 2D copper-water nanofluid flow squeezed between two parallel plates is considered in this paper. Both plates are set in a porous medium and assumed that the porous medium is both thermally and hydro-dynamically isotropic. The coordinate axes X and Y are taken through the plate and at right angles to the plates respectively as given in Figure 1. The gap between the plates at any instant t is $h(t) = H(1-at)^{0.5}$ where H the position of the plates at $t = 0$ and a is named as characteristic parameter with dimension $\frac{1}{t}$. Here $a > 0$ denotes both plates are approaching one another (squeezing moment) with velocity $v(t) = h'(t)$ till the plates meet one another at $t = 1/a$ whereas $a < 0$ indicates the outward motion of the plates. A magnetic field of intensity $B(t) = B_0(1-at)^{-0.5}$ is exerted in the direction normal to the fluid flow i.e along the y axis and B_0 is the initial intensity of the magnetic field i.e at $t = 0$. The component of the nanofluid considered in this problem is copper-water. Physical characteristics of the nanofluid components are specified below as Table 1.

Table 1 Physical Characteristics of Components of the Nanofluid

Thermal Conductivity (W/mK)	Density (kg/m ³)	Specific heat capacity (J/kg K)
Copper 8933	385	401
Pure water 997.1	4179	0.613

The mathematical model of the problem is constructed with the assumptions that (i) the porous medium is both thermally and hydrodynamically

isotropic (ii) no slip among the plates (iii) thermal equilibrium occurs between the base liquid and the nanoparticle (iv) radiative heat transfer takes place (v) no chemical reaction between the components of the nanofluid and (vi) physical characteristics of nanoparticle and base fluid are constants. The incompressible boundary layer squeezing flow of nanofluid along with heat transfer is governed by the continuity, momentum and energy equations (1) - (4) given below.

$$\frac{\partial u}{\partial x} + \frac{\partial v}{\partial y} = 0 \tag{1}$$

$$\rho_{nf} \left(\frac{\partial u}{\partial t} + u \frac{\partial u}{\partial x} + v \frac{\partial u}{\partial y} \right) = -\frac{\partial p}{\partial x} + \mu_{nf} \left(\frac{\partial^2 u}{\partial x^2} + \frac{\partial^2 u}{\partial y^2} \right) - \sigma_{nf} B^2(t) u - \frac{\mu_{nf} u}{k_p} \tag{2}$$

$$\rho_{nf} \left(\frac{\partial v}{\partial t} + u \frac{\partial v}{\partial x} + v \frac{\partial v}{\partial y} \right) = -\frac{\partial p}{\partial y} + \mu_{nf} \left(\frac{\partial^2 v}{\partial x^2} + \frac{\partial^2 v}{\partial y^2} \right) - \frac{\mu_{nf} v}{k_p} \tag{3}$$

$$\frac{\partial T}{\partial t} + u \frac{\partial T}{\partial x} + v \frac{\partial T}{\partial y} = \frac{K_{nf}}{(\rho C_p)_{nf}} \left(\frac{\partial^2 T}{\partial x^2} + \frac{\partial^2 T}{\partial y^2} \right) + \frac{\mu_{nf}}{(\rho C_p)_{nf}} \left[4 \left(\frac{\partial u}{\partial x} \right)^2 + \left(\frac{\partial u}{\partial y} + \frac{\partial v}{\partial x} \right)^2 \right] + \frac{1}{(\rho C_p)_{nf}} \frac{16\sigma^* T_0^3}{3k'} \left[\frac{\partial^2 T}{\partial x^2} + \frac{\partial^2 T}{\partial y^2} \right] \tag{4}$$

Here the velocity components along the axes x and y are denoted by u and v respectively. P, T, k' and σ^* represent the pressure, the temperature, the coefficient of mean absorption & the constant due to Stefan-Boltzmann. K_{nf} , ρ_{nf} , μ_{nf} , and $(\rho C_p)_{nf}$

represent the effective thermal conductivity, effective density, effective dynamic viscosity and effective specific heat capacity of the nanoliquid respectively. The base liquid and the nanoparticles are connected by the relations as follows.

$$\rho_{nf} = (1 - \phi)\rho_f + \phi\rho_s \tag{5}$$

$$\mu_{nf} = \frac{\mu_f}{(1 - \phi)^{2.5}} \tag{6}$$

$$K_{nf} = K_f \frac{2K_f + K_s - 2\phi(K_f - K_s)}{2K_f + K_s + \phi(K_f - K_s)} \tag{7}$$

$$(\rho C_p)_{nf} = \phi(\rho C_p)_s + (1 - \phi)(\rho C_p)_f \tag{8}$$

$$\sigma_{nf} = \sigma_f \left[1 + \frac{3\{(\sigma_s \sigma_f^{-1}) - 1\}\phi}{\{(\sigma_s \sigma_f^{-1}) + 2\}\phi - \{(\sigma_s \sigma_f^{-1}) - 1\}\phi} \right] \tag{9}$$

The boundary settings are as follows:

$$\left. \begin{aligned} u = 0, \quad v = \frac{dh}{dt}, \quad -k \frac{\partial T}{\partial y} = h_f (T_f - T) \quad \text{at} \quad y = h(t) \\ \frac{\partial u}{\partial y} = 0, \quad v = 0, \quad \frac{\partial T}{\partial y} = 0 \quad \text{at} \quad y = 0 \end{aligned} \right\} \quad (10)$$

During conversion of the primary eqns.(1)-(4) into ODEs, η - the similarity variable, h and θ - the dimensionless functions are introduced as below:

$$\left. \begin{aligned} u = \frac{ax}{2(1-at)} g'(\eta), \quad v = \frac{-aH}{2\sqrt{1-at}} g(\eta) \\ \eta = \frac{y}{H\sqrt{1-at}}, \quad \theta = \frac{T - T_H}{T_f - T_H}, \quad B(t) = B_o (1-at)^{-0.5} \end{aligned} \right\} \quad (11)$$

Applying similarity transformation and dimensionless functions in eqns. (2), (3) and (4), after removing pressure gradients the following equations are obtained.

$$g^{IV} - A_1 S (1-\phi)^{2.5} [3g'' + \eta g''' + g'g'' - gg'''] - \left(M + \frac{1}{Da} \right) g'' = 0 \quad (12)$$

$$\left(1 + \frac{4}{3} R_d \right) \theta'' + \text{Pr} S \left(\frac{A_2}{A_3} \right) (g\theta' - \eta\theta') + \frac{P_r E_c}{A_3 (1-\phi)^{2.5}} [g''^2 + 4\delta^2 g'^2] = 0 \quad (13)$$

The accompanying limiting conditions are,

$$\left. \begin{aligned} g(0) = 0, \quad g''(0) = 0, \quad \theta'(0) = 0 \quad \text{at} \quad \eta = 0 \\ g(1) = 1, \quad g'(1) = 0, \quad \theta'(1) = Bi[\theta(1) - 1] \quad \text{at} \quad \eta = 1 \end{aligned} \right\} \quad (14)$$

Where

- $A_1 = (1-\phi) + \phi \frac{\rho_s}{\rho_f}$,
- $A_2 = (1-\phi) + \phi \frac{(\rho C_p)_s}{(\rho C_p)_f}$,
- $A_3 = \frac{2k_f + k_s - 2\phi(k_f - k_s)}{2k_f + k_s + \phi(k_f - k_s)} \text{Pr} = \frac{(\rho C_p)_f \mu_f}{k_f \rho_f}$ is the Prandtl number,
- $Ec = \frac{\rho_f}{(\rho C_p)_f (T_f - T_H)} \left(\frac{ax}{2(1-at)} \right)^2$ is the modified Eckert number,
- $M = \frac{\sigma_s H^2 B_o^2}{\mu_{nf}}$ is the Hartmann number,

- $Da = \frac{k_p}{H^2}$ is the Darcy number,
- $R_d = \frac{4\sigma^* T_o^3}{A_3 k_f k'}$ is the thermal radiation parameter,
- $\delta = \frac{H\sqrt{1-at}}{x}$ is the dimensionless length
- $Bi = \frac{h_f h(t)}{k}$ is the Biot number,
- $S = \frac{aH^2}{2\nu_f}$ is the squeeze number

Which can be negative or positive. Negative sign of S represents the plates are coming close to one

another and the plates are moving away from one another when S is positive. ν_f is the kinematic viscosity.

2. Solution Procedure - Differential Transformation Method (DTM)

Differential transformation method is an assured technique to resolve both nonlinear and linear ODEs, PDEs and is not influenced by the result of any round off errors. $f(t)$ be an analytic function defined in the time domain I and let $t_0 \in I$. Then $f(t)$ can be written as a power series about t_0 and the differential transform of $f(t)$ is given by,

$$F(n) = \frac{1}{n!} \left. \frac{d^n f(t)}{dt^n} \right|_{t=t_0} \quad (15)$$

where $F(n)$ is called the transformed function of $f(t)$. The inverse differential transform of $F(n)$ is defined as below:

$$\delta(q) = \begin{cases} 1 & \text{if } q = 1 \\ 0 & \text{if } q \neq 1 \end{cases}, \text{ yields}$$

Applying DTM in equation (12) with

$$\left. \begin{aligned} &(\lambda + 1)(\lambda + 2)(\lambda + 3)(\lambda + 4)G[\lambda + 4] - 3A_1S(1 - \phi)^{2.5}(\lambda + 1)(\lambda + 2)G[\lambda + 2] \\ &- A_1S(1 - \phi)^{2.5} \sum_{q=0}^{\lambda} \delta(\lambda - q - 1)(q + 1)(q + 2)(q + 3)G[q + 3] \\ &- A_1S(1 - \phi)^{2.5} \sum_{q=0}^{\lambda} (\lambda - q + 1)G[\lambda - q + 1](q + 1)(q + 2)G[q + 2] \\ &+ A_1S(1 - \phi)^{2.5} \sum_{q=0}^{\lambda} G[\lambda - q](q + 1)(q + 2)(q + 3)G[q + 3] - \left(M + \frac{1}{Da}\right)(\lambda + 1)(\lambda + 2)G[\lambda + 2] = 0 \end{aligned} \right\} \quad (18)$$

The corresponding transformed limiting conditions are given as below:

$$G[0] = 0, \quad G[1] = C_1, \quad G[2] = 0, \quad G[3] = C_2 \quad (19)$$

Where C_1 and C_2 are constants.

The iterated limiting conditions $G[\lambda]$ are obtained as follows:

$$G[5] = \left. \begin{aligned} &G[0] = 0, \quad G[1] = C_1, \quad G[2] = 0, \quad G[3] = C_2, \quad G[4] = 0 \\ &G[5] = \left[\frac{3}{20} S A_1 (1 - \phi)^{2.5} + \frac{1}{20} \left(M + \frac{1}{Da} \right) \right] C_2, \quad G[6] = \frac{1}{60} S A_1 (1 - \phi)^{2.5} C_2 \end{aligned} \right\} \quad (20)$$

$$f(t) = \sum_{n=0}^{\infty} F(n)(t - t_0)^n \quad (16)$$

From equations (19) and (20) we have $f(t)$ as below:

$$f(t) = \sum_{n=0}^{\infty} \frac{1}{n!} \left[\frac{d^n f(t)}{dt^n} \right]_{t=t_0} (t - t_0)^n \quad (17)$$

Table 2 Standard Differential Transforms

S. No	Given Function	Transformed Function
1	$g(t) = ag_1(t) \pm bg_2(t)$	$g(\lambda) = ag_1(\lambda) \pm bg_2(\lambda)$
2	$g(t) = \frac{d^r g(t)}{dt^r}$	$g(\lambda) = \frac{(\lambda + r)!}{\lambda!} g(\lambda + r)$
3	$g(t) = g_1(t) \cdot g_2(t)$	$g(\lambda) = \sum_{p=0}^{\lambda} G_1(p) \cdot G_2(\lambda - p)$
4	$g(t) = t^r$	$g(\lambda) = \delta(\lambda - r) = \begin{cases} 1 & \text{if } \lambda = r \\ 0 & \text{if } \lambda \neq r \end{cases}$

Using eqn. (17),
$$g(\eta) = \sum_{\lambda=0}^{\infty} G[\lambda] \eta^\lambda \tag{21}$$

Eqns. (20) and (21) results in

$$g(\eta) = C_1 \eta + C_2 \eta^3 + \left[\frac{3}{20} SA_1 (1-\phi)^{2.5} + \frac{1}{20} \left(M + \frac{1}{Da} \right) \right] C_2 \eta^5 + \frac{1}{60} SA_1 (1-\phi)^{2.5} C_2 \eta^6 + \dots \tag{22}$$

Applying DTM in eqn. (13) yields

$$\begin{aligned} & \left(1 + \frac{4}{3} R_d \right) (\lambda + 1)(\lambda + 2) \Theta[\lambda + 2] + S \Pr \left(\frac{A_2}{A_3} \right) \sum_{q=0}^{\lambda} G[\lambda - q](q + 1) \Theta[q + 1] - S \Pr \left(\frac{A_2}{A_3} \right) \\ & \sum_{q=0}^{\lambda} \delta [\lambda - q - 1](q + 1) \Theta[q + 1] + \frac{\Pr Ec}{A_3 (1-\phi)^{2.5}} \sum_{q=0}^{\lambda} (\lambda - q + 1)(\lambda - q + 2) G[\lambda - q + 2] \\ & (q + 1)(q + 2) G[q + 2] + \frac{4 \Pr Ec \delta^2}{A_3 (1-\phi)^{2.5}} \sum_{q=0}^{\lambda} (\lambda - q - 1) G[\lambda - q + 1](q + 1) G[q + 1] = 0 \end{aligned} \tag{23}$$

The corresponding limiting values are

$$\Theta[0] = C_3, \quad \Theta[1] = 0 \tag{24}$$

Here C_3 - a constant. Using the limiting conditions $\Theta[\lambda]$ are obtained as follows:

$$\left. \begin{aligned} \Theta[0] = C_3, \quad \Theta[1] = 0, \quad \Theta[2] = \frac{-2 \Pr Ec \delta^2}{A_3 (1-\phi)^{2.5}} \frac{C_1^2}{\left(1 + \frac{4}{3} R_d \right)}, \quad \Theta[3] = 0 \\ \Theta[4] = S \Pr \left(\frac{A_2}{A_3} \right) \left(\frac{-C_1}{6 \left(1 + \frac{4}{3} R_d \right)} \right) \Theta[2] - \frac{\Pr Ec}{A_3 (1-\phi)^{2.5}} [3C_2^2 + 2\delta^2 C_1 C_2] \end{aligned} \right\} \tag{25}$$

Using eqn (20),
$$\theta(\eta) = \sum_{\lambda=0}^{\infty} \Theta[\lambda] \eta^\lambda \tag{26}$$

Eqns. (29) and (30) results in

$$\theta[\eta] = C_3 + \left(\frac{-2 \Pr Ec \delta^2 C_1^2}{A_3 (1-\phi)^{2.5} \left(1 + \frac{4}{3} R_d \right)} \right) \eta^2 + \left[S \Pr \left(\frac{A_2}{A_3} \right) \left(\frac{-C_1}{6 \left(1 + \frac{4}{3} R_d \right)} \right) \Theta[2] - \frac{\Pr Ec}{A_3 (1-\phi)^{2.5}} [3C_2^2 + 2\delta^2 C_1 C_2] \right] \eta^4 + \dots \tag{27}$$

Taking $\eta = 1, \Pr = 6.7, S = 0.5, Ec = 0.1, M = 1.5, \delta = 0.1, \phi = 0.01, Da = 0.1$ in eqns. (26), (31) and from Table 1 the constants C_1, C_2 and C_3 can be evaluated.

3. Results and Discussion

This work presents details pertaining to the progress of a mathematical representation of copper-water nanofluid flow squeezed between parallel plates in a porous medium as presented in figure 1. The significant consequences of thermal radiation together with related parameters like squeezing number, Hartmann number, Darcy number, Eckert number, and Biot number on the profiles of flow behavior and temperature of copper-water nanofluid system are discussed with the help of tables and graphs. While replicating the model the values for the parameters are fixed as follows:

$$Pr = 6.7, \phi = 0.03, M = 2, R_d = 2, Ec = 0.5, Da = 0.1, \delta = 0.1, \text{ and } \beta = 4.$$

Figures 2 (a) and 2(b) describe the consequence of squeezing parameter S on velocity f' and temperature θ of the copper-water nanofluid. From the figures it can be concluded that the velocity and temperature values are slightly less for every value of S , and the overall spread in velocity is reduced and not significant in temperature values when compared to the outcomes of [15] in which the authors investigated the case where the radiation term and porous medium were absent. Figure 2(a) shows that f' come down for enhancing S for each η over $0 \leq \eta \leq 0.49$ (approx.) and starts increasing for the values of η in $0.49 < \eta \leq 1$. As a consequence of reduce in fluid flow next to the boundary area the velocity gradient increases there. While retaining the conventional mass flow rate, the reduced fluid flows close to the border line of the plates are balanced by the greater fluid flows close to the middle region. As a result, a separation point occurs at $\eta = 0.49$. Figure 2(b) depicts the consequences of squeezing number on the temperature of the copper-water system for various values of S . With enhancing squeeze number S the corresponding θ values decreases steadily for the values of η between 0 & 1. When S is maximum the kinematic viscosity becomes minimum, which makes higher the speed rate of separation of the plates. Hence the contact pressure is reduced between the plates that results in reduced temperature of the nanofluid.

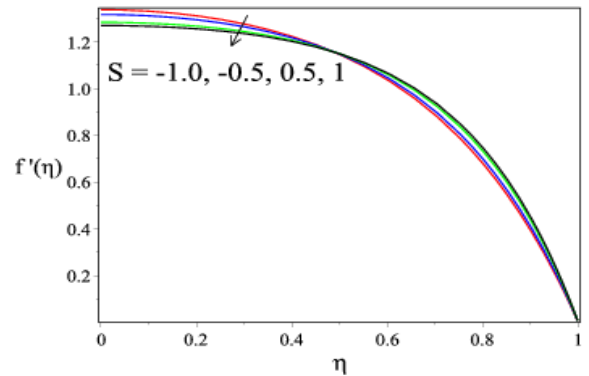


Figure 2(a) Effect of S on f'

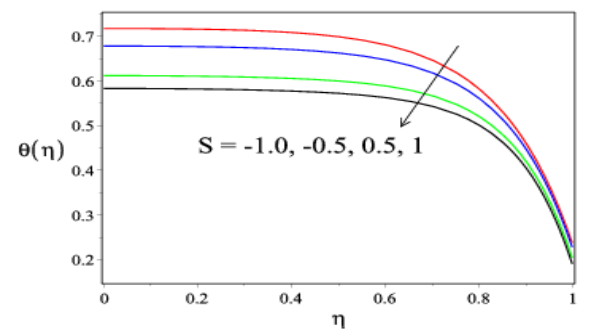


Figure 2(b) Effect of S on θ

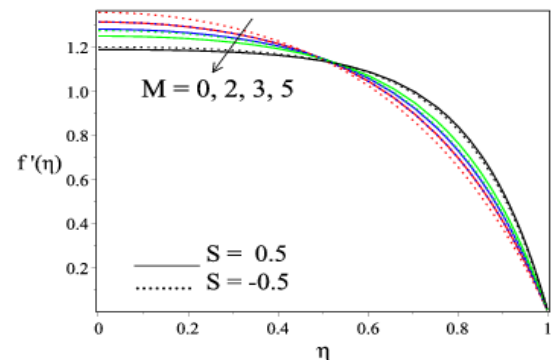


Figure 3(a) Effect of M on f'

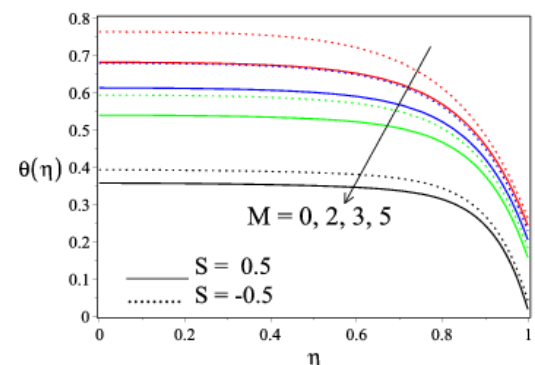


Figure 3(b) Effect of M on θ

Figures 3(a) & 3(b) show the influences of Hartmann number M on velocity f' and temperature field θ of the nanofluid. From figure 3(a), it is noted that for both $S = 0.5$ & $S = -0.5$, as M increases correspondingly f' decreases between the area $\eta = 0$ & $\eta = 0.49$ and starts increasing between the region $\eta > 0.49$ & $\eta \leq 1$. With existing thermal radiation, a raise in Hartmann number is associated with raise in magnetic field and a power called Lorentz force is generated that reduces the fluid movement in the region closure to the boundary during squeezing movement. Moreover when the plates are moving closure to each other, the consequence of Lorentz force is found to be very less. Zero velocity is attained at $\eta = 1$ due to skin friction that stops the flow of nanofluid. Also from the graph plotted showing variation in velocity, the cross over point occurs at $\eta = 0.49$ and the velocity of the nanofluid for $S = -0.5$ is greater when compared to $S = 0.5$ in the region $0 \leq \eta \leq 0.49$ and an opposite trend in $0.49 < \eta \leq 1$. Table 2 explains that with enhancing M , the dimensionless skin friction reduces. Figure 3(b) portrays that for both $S = 0.5$ and $S = -0.5$ the temperature values turn down with increasing M . But the influence on temperature is lesser for $S = 0.5$ than $S = -0.5$. Figures 3(a) & 3(b) exhibit, with existing radiation parameter the spread in velocity and temperature values are enhanced and the values are greater to some extent for all the values of S in comparison with [15]. Figures 4(a) and 4(b) present the impact of Darcy number Da on the nanofluid's flow behavior f' and temperature θ . A decrease in Darcy number implies lower permeability, which in turn increases the resistance to fluid flow. It is viewed from figure 4(a) that the fluid flow raises with enhance in Darcy number. When the Darcy number is very low, f' is constant over $0 \leq \eta \leq 0.6$ and the values beyond $\eta = 0.6$ decreases rapidly and becomes zero near the boundary of the plate. As Da raises, the flow is more concentrated in the center and the velocity decreases steadily from the center to the end of the plate, also with the effect of skin friction velocity becomes low near the boundary. Figure 4(b) depicts the effect of variation in Da on temperature profile. Increasing Darcy number results in higher

temperature. The temperature enhances with enhancing Darcy number for both $S = 0.5$ & $S = -0.5$ and increase in temperature values corresponding to $S = -0.5$ are greater than for $S = 0.5$.

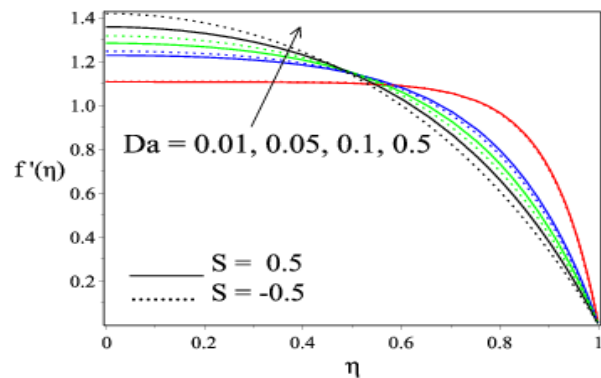


Figure 4(a) Effect of Da on f'

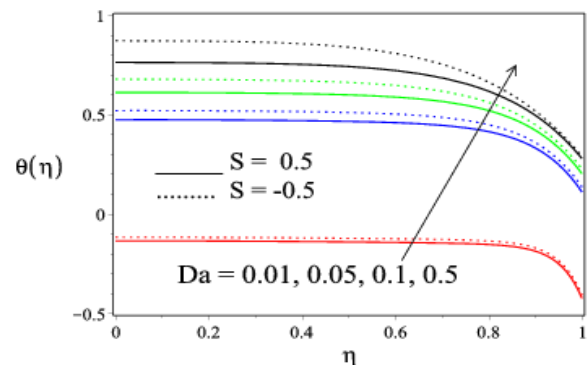


Figure 4(b) Effect of Da on θ

Figure 5 depicts the consequences of Eckert number Ec on temperature θ . With increasing Ec the temperature decreases for both $S = 0.5$ & $S = -0.5$. But the values of temperature corresponding to $S = 0.5$ are less than the values corresponding to $S = -0.5$ for each value of Ec . While comparing the effect with [15] the spread in temperature values attained in the present work for both $S = 0.5$ and $S = -0.5$ are less and this can be attributed to the existence of thermal radiation. The influence of radiation parameter R_d on temperature θ is shown in figure 6 through which it follows that as R_d increases, θ also increases for both $S = 0.5$ & $S = -0.5$. This is owing to the existence of thermal radiation the temperature of the entire fluid flow

area enhances. Generally, it is true that increase in the Rosseland diffusion approximation for radiation enhances the fluid temperature, and hence the distribution of temperature shows greater values of θ for greater values of R_d . The temperatures are seen to decrease closer to the plate ($\eta = 1$) and this can be due to the conduction of heat from the plates.

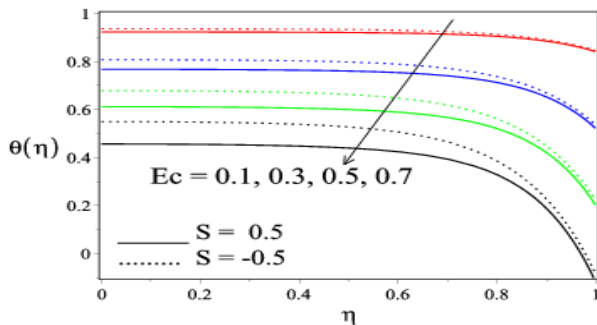


Figure 5 Effect of Ec on θ

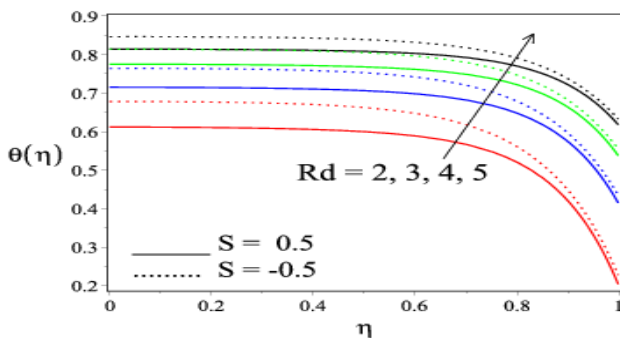


Figure 6 Effect of R_d on θ

The effect of β - the Biot number on temperature field θ is presented in figure 7. For both $S = 0.5$ and $S = -0.5$ the temperature profile θ raises for enhancing β and the temperature values corresponding to $S = -0.5$ are greater than those for values corresponding to $S = 0.5$. As the Biot number β is involving the heat transfer coefficient, increasing values of β implies reduced thermal conductivity giving rise to higher temperature. Figure 8 depicts the effect of R_d and β on Nu - the Nusselt number. Augmenting values of β and R_d the heat transfer values corresponding to $S = 0.5$ are increasing whereas the values corresponding to $S = -0.5$ are decreasing. Moreover, for both $S = 0.5$ and $S = -0.5$,

the heat transfer values do not vary for the given values of R_d .

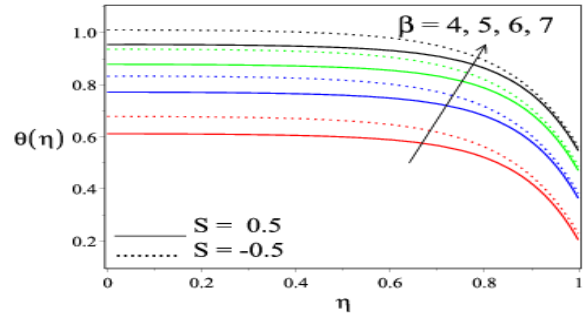


Figure 7 Effect of β on θ

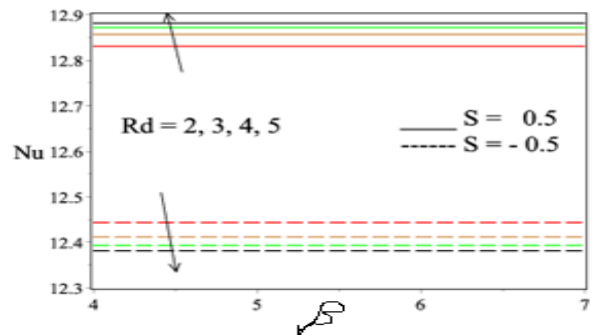


Figure 8 Effects of R_d & β on Nu

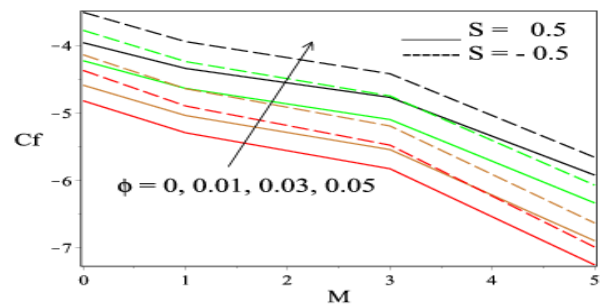


Figure 9(a) Effects of ϕ & M on C_f

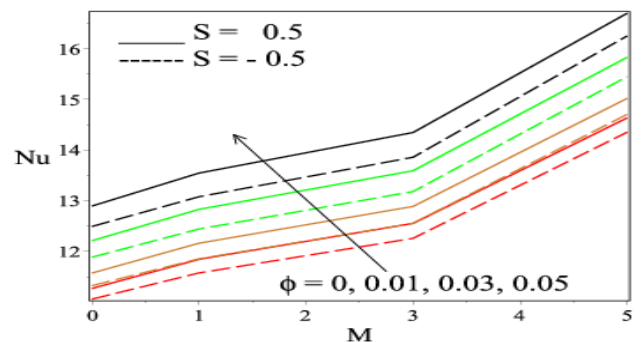


Figure 9(b) Effects of ϕ & M on Nu

Figures 9(a) & 9(b) present the influences of variation in volume fraction ϕ and M on skin friction & Nusselt number respectively. It reveals from figure 9(a) that with increasing ϕ the value of C_f is seen to increase whereas with increasing M , represents the magnetic field strength causing slow movement of the nanofluid, the skin friction C_f comes down for both $S = -0.5$ and $S = 0.5$. The values of C_f are lower for $S = 0.5$ compared to the values corresponding to $S = -0.5$ and also the differences in values between $S = 0.5$ and $S = -0.5$ are less significant. Figure 9(b) shows that with increasing ϕ and M the values of local heat transfer Nu turns high for both $S = -0.5$ and $S = 0.5$. From the figures it is found that the slope of the graph connecting C_f and M the values are gradually decreasing and, in the graph, connecting Nu & M , the values are gradually increasing for $S = 0.5$ and $S = -0.5$ as well.

Conclusion

In the current study, the consequence of radiation parameter on the temperature profiles and flow behavior of the copper-water nanofluid squeezed between parallel plates in a porous medium is analyzed. By means of similarity transformation, the primary PDEs are transformed into nonlinear ODEs which are resolved analytically using DTM and the outcomes are conferred with the help of graphs and tables are compared with results of [15]. The following conclusions are observed based on the resultant solutions through our investigation.

- The velocity and temperature values reduced while enhancing both squeezing and Hartmann numbers and as a result, the non-dimensional skin friction reduces steadily for $S = 0.5$ and $S = -0.5$.
- With increasing Darcy numbers, the temperatures as well as the velocity increase for given S .
- With increase in radiation parameter the temperature values raised and these temperature values are comparatively less for $S = 0.5$ than $S = -0.5$.

References

[1]. J. Engmann, C. Servais, A.S. Burbidge, Squeeze flow theory and applications to rheometry: A review. Journal

of Non-Newtonian Fluid Mechanics, Vol. 132, (2005) 1-27.

- [2]. S. Sivasankaran, C. J. Ho, Effect of temperature dependent properties on MHD convection of water near its density maximum in a cavity. International Journal of Thermal Sciences, Vol. 47, (2008) 1184-1194.
- [3]. S. Sivasankaran, M. Bhuvanewari, Y.J. Kim, C.J. Ho, K.L. Pan, Magneto-convection of cold water near its density maximum in an open cavity with variable fluid properties. International Journal of Heat Fluid Flow, Vol. 32, (2011) 932 – 942.
- [4]. R. Bindhu, G. Sai SundaraKrishnan, S. Sivasankaran, M. Bhuvanewari, Magneto-convection of water near its maximum density in a cavity with partially thermally active walls. Energy & Environment, Vol. 30, (2019) 833-853.
- [5]. S. Sivasankaran, A. Malleswaran, J. Lee, P.Sundar, Hydro-magnetic combined convection in a lid-driven cavity with sinusoidal boundary conditions on both sidewalls. International Journal of Heat Mass Transfer, Vol. 54, (2011) 512-525.
- [6]. A. Malleswaran, S. Sivasankaran, M. Bhuvanewari, Effect of heating location and size on MHD convection in a lid-driven cavity. International Journal of Numerical Methods Heat Fluid Flow, Vol. 23, (2013) 867-884.
- [7]. S. Sivasankaran, M.A. Mansour, A.M. Rashad, M. Bhuvanewari, MHD mixed convection of Cu– water nanofluid in a two-sided lid-driven porous cavity with a partial slip. Numerical Heat Transfer; Part A: Applications, Vol. 70, (2016) 1356-1370.
- [8]. S. Sivasankaran, K. Narrein, Influence of geometry and magnetic field on convective flow of nanofluids in trapezoidal microchannel heat sink. Iran Journal of Science and Technology Transactions on



- Mechanical Engineering, Vol. 44, (2020) 373–382.
- [9]. A.M. Siddiqui, S. Irum, A.R. Ansari, Unsteady squeezing flow of a viscous MHD fluid between parallel plates a solution using the homotopy perturbation method. *Mathematical Modeling and Analysis*, Vol. 13, (2008) 565-576.
- [10]. A. Saadatmandi, A. Asadi, A. Eftekhari, Collocation method using quintic B-spline and sinc functions for solving a model of squeezing flow between two infinite plates. *International Journal of Computer Mathematics*, Vol. 93, (2016) 1921-1936.
- [11]. X.J. Ran, Q.Y. Zhu, Y. Li, An explicit series solution of the squeezing flow between two infinite plates by means of the homotopy analysis method. *Communications in non-linear Science and Numerical Simulation*, Vol. 14, (2009) 119-132.
- [12]. M.M. Rashidi, A.M. Siddiqui, M.T. Rastegari, Analytical solution of squeezing flow between two circular plates. *International Journal for Computational Methods in Engineering Science and Mechanics*, Vol. 13, (2012) 342-349.
- [13]. A. Dib, A. Haiahem, B. Bou-said, Approximate analytical solution of squeezing unsteady nanofluid flow. *Powder Technology*, Vol. 269, (2015) 193–199.
- [14]. U. Khan, N. Ahmed, M. Asadullah, S.T. Mohyud-din, Effects of viscous dissipation and slip velocity on two-dimensional and axisymmetric squeezing flow of Cu-water and Cu-kerosene nanofluids. *Propulsion and power research*, Vol.4, (2015) 40 – 49.
- [15]. N. Acharya, K. Das, P. K. Kundu, The squeezing flow of Cu-water and Cu-kerosene nanofluids between two parallel plates. *Alexandria Engineering Journal*, Vol. 55, (2016) 1177-1786.
- [16]. A. Noghrehabadi, R. Pourrajab, M. Ghalambaz, Flow and heat transfer of nanofluids over stretching sheet taking into account partial slip and thermal convective boundary conditions. *Heat Mass Transfer* Vol. 49, (2013) 1357–1366.
- [17]. A. Noghrehabadi, M. R. Saffarian, R. Pourrajab, M. Ghalambaz, Entropy analysis for nanofluid flow over a stretching sheet in the presence of heat generation/absorption and partial slip. *Journal of Mechanical Science and Technology*, Vol.27, (2013) 927-937.
- [18]. T. Hayat, M. Imtiaz, A. Alsaedi, R. Mansoor, MHD flow of nanofluids over an exponentially stretching sheet in a porous medium with convective boundary conditions. *Chin. Phys. B* Vol. 23, (2014) 054701.
- [19]. O.D. Makinde, A. Aziz, Boundary layer flow of a nanofluid past a stretching sheet with a convective boundary condition. *International Journal of Thermal Sciences*, Vol. 50, (2011) 1326-1332.
- [20]. W. A. Khan, R. S. R. Gorla, Heat and mass transfer in power-law nanofluids over a nonisothermal stretching wall with convective boundary condition. *Journal of heat transfer*, Vol. 134, (2012).112001 (1-7)
- [21]. A. Aziz, W.A. Khan, Natural convective boundary layer flow of a nanofluid past a convectively heated vertical plate. *International Journal of Thermal Sciences*, Vol. 52,(2012) 83-90.
- [22]. M.H. Mkwizu, O.D. Makinde, Entropy generation in a variable viscosity channel flow of nanofluids with convective cooling. *Comptes Rendus Mecanique*, Vol. 343(1), 2015, 38-56.
- [23]. H. Niranjana, S. Sivasankaran, M. Bhuvaneshwari, Analytical and Numerical Study on magnetoconvection stagnation-point flow in a porous medium with chemical reaction, radiation and slip effects. *Mathematical Problems in Engineering*, Vol. 2016, (2016) 1-12.
- [24]. H. Niranjana, S. Sivasankaran, M. Bhuvaneshwari, Chemical reaction, soot and dufour effects on MHD mixed



- convection stagnation point flow with radiation and slip condition. *ScientiaIranica – B Mechanical Engineering*, Vol. 24, (2017) 698-706.
- [25]. S. Sivasankaran, H. Niranjana, M. Bhuvaneshwari, Chemical reaction, radiation and slip effects on MHD mixed convection stagnation-point flow in a porous medium with convective boundary condition. *International Journal of Numerical Methods for Heat & Fluid Flow*, Vol. 27, (2017) 454-470.
- [26]. S. Karthikeyan, M. Bhuvaneshwari, S. Sivasankaran, S. Rajan, Soret and Dufour effects on MHD mixed convection heat and mass transfer of a stagnation point flow towards a vertical plate in a porous medium with chemical reaction, radiation and heat generation. *Journal of Applied Fluid Mechanics*, Vol. 9, (2016) 1447-1455.
- [27]. M. Farooq, S. Ahmad, M. Javed, A. Anjum, Analysis of Cattaneo-Christov heat and mass fluxes in the squeezed flow embedded in porous medium with variable mass diffusivity. *Results in Physics*, Vol. 7, (2017) 3788–3796.
- [28]. S. Mohyud-din, S.I. Khan, U. Khan, N. Ahmed, Y. Xiao-jun, Squeezing flow of MHD fluid between parallel disks. *International Journal for Computational Methods in Engineering Science and Mechanics*, Vol. 19, (2018) 42-47.
- [29]. A. Kasaeian, R.D. Azarian, O. Mahian, L.Kolsi, A. J. Chamkha, S. Wongwises, L. Pop, Nanofluid flow and heat transfer in porous media: A review of the latest developments. *International Journal of Heat and Mass Transfer*, Vol.107, (2017) 778-791.
- [30]. A. K. Pandey, M. Kumar, Squeezing unsteady MHD Cu-water nanofluid flow between two parallel plates in porous medium with suction/injection. *Computational and Applied Mathematics Journal*, Vol.4, (2018) 31-42.
- [31]. M. G. Sobamow, A. T. Akinshilo, A. A. Yinusa, Thermo-magneto-solutal squeezing flow of nanofluid between two parallel disks embedded in a porous medium: Effects of nanoparticle geometry, slip and temperature jump conditions. *Modelling and Simulation in Engineering*, Vol. 2018, (2018) Article ID 7364634.
- [32]. M.G. Sobamowo, A. A. Yinusa, S.T. Aladenusi, Impacts of magnetic field and thermal radiation on squeezing flow and heat transfer of third grade nanofluid between two disks embedded in a porous medium. *Heliyon*, Vol. 6, (2020) e03621.